FIRST RESULTS FROM SOHO

B. FLECK
ESA Space Science Department, NASA/GSFC, Greenbelt, Maryland, USA

Abstract. SOHO, the Solar and Heliospheric Observatory, is a project of international cooperation between ESA and NASA to study the Sun, from its deep core to the outer corona, and the solar wind. Three helioseismology instruments are providing unique data for the study of the structure and dynamics of the solar interior, from the very deep core to the outermost layers of the convection zone. A set of five complementary remote sensing instruments, consisting of EUV, UV and visible light imagers, spectrographs and coronagraphs, give us our first comprehensive view of the outer solar atmosphere and corona, leading to a better understanding of the enigmatic coronal heating and solar wind acceleration processes. Finally, three experiments complement the remote sensing observations by making in-situ measurements of the composition and energy of the solar wind and charged energetic particles, and another instrument maps the neutral hydrogen in the heliosphere and its dynamic change by the solar wind. This paper reports some of the first results from the SOHO mission.

1. Introduction

SOHO, the Solar and Heliospheric Observatory, is a project of international co-operation between ESA and NASA to study the Sun, from its deep core to the outer corona, and the solar wind (Domingo *et al.*, 1995). It carries a complement of twelve sophisticated, state-of-the-art instruments (see Table I), developed and furnished by twelve international PI consortia involving 39 institutes from fifteen countries (Belgium, Denmark, Finland, France, Germany, Ireland, Italy, Japan, Netherlands, Norway, Russia, Spain, Switzerland, United Kingdom, and the United States). Detailed descriptions of all the twelve instruments on board SOHO as well as a description of the SOHO ground system, science operations and data products together with a mission overview can be found in Fleck *et al.* (1995).

SOHO was launched by an Atlas II-AS from Cape Canaveral Air Station on 2 December 1995, and was inserted into its halo orbit around the L1 Lagrangian point on February 14, 6 weeks ahead of schedule. Commissioning of the spacecraft and the scientific payload was completed end of March 1996. The launch was so accurate and the orbital manoeuvres were so efficient that there remains sufficient fuel on board to maintain the halo orbit for several decades, several times the time originally foreseen (up to six years).

In the following sections some of the new results from the various SOHO instruments are presented, starting with the Sun's interior and working out to the solar wind at L1.

Astrophysics and Space Science **258:** 57–75, 1998.

TABLE I
The SOHO Scientific Instruments

Investigation		Principal Investigator
GOLF	Global Oscillations at Low Frequencies	A. Gabriel, IAS, Orsay, France
VIRGO	Variability of Solar Irradiance and Gravity Oscillations	C. Fröhlich, PMOD Davos, Switzerland
MDI/SOI	Michelson Doppler Imager / Solar Oscillations Investigation	P. Scherrer, Stanford University, USA
SUMER	Solar Ultraviolet Measurements of Emitted Radiation	K. Wilhelm, MPAe Lindau, Germany
CDS	Coronal Diagnostic Spectrometer	R. Harrison, RAL, Chilton, England
EIT	Extreme-ultraviolet Imaging Telescope	J.-P. Delaboudinière, IAS, Orsay, France
UVCS	UltraViolet Coronagraph Spectrometer	J. Kohl, SAO, Cambridge, USA
LASCO	Large Angle Spectroscopic COronagraph	G. Brueckner, NRL, Washington, USA
SWAN	Solar Wind ANisotropies	J.-L. Bertaux, SA, Verrières, France
CELIAS	Charge, Element and Isotope Analysis System	P. Bochsler, Univ. Bern, Switzerland
COSTEP	COmprehensive SupraThermal and Energetic Particle analyzer	H. Kunow, Univ. Kiel, Germany
ERNE	Energetic and Relativistic Nuclei and Electron experiment	J. Torsti, Univ. Turku, Finland

2. The Solar Interior

Just as seismology reveals the Earth's interior by studying earthquake waves, solar physicists are probing inside the Sun using a technique called 'helioseismology'. Oscillations detectable at the visible surface are due to sound waves reverberating through the Sun's interior. These oscillations are usually described in terms of normal modes that are identified by three integers: angular degree l, angular order m, and radial order n. The frequencies of the normal modes depend on the structure and flows in the regions where the modes propagate. Because different modes sample different regions inside the Sun, by observing many modes one can, in principle, map the solar interior.

The main goal of helioseismology is to infer the structure and dynamics of the Sun's interior from the oscillation frequencies of normal modes. Obviously, the resolving power of these inferences depends mainly on the accuracy and precision of the measurements of these frequencies as well as on the bandwidth (number) of the normal modes measured, both in degree l and in order n.

The three helioseismology instruments (GOLF, VIRGO, MDI) on board SOHO are harvesting the benefit of the extremely stable platform that the SOHO space-

craft provides above the disturbing Earth's atmosphere, and, equally important, of the continuous, uninterrupted measurements allowed by the unique orbit around L1. Already now, with a time series of less than one year duration, GOLF (Gabriel *et al.*, 1995) measurements of the global (low degree) velocity oscillations of the sun have shown a factor of 10 improvement over that available from ground-based observations demonstrating the difficulty of making precise measurements through the earth's disturbing atmosphere (Gabriel, priv. comm.). The resulting high-precision measurements of the sound speed for the central region of the Sun puts severe constraints on the existing theoretical models of the Sun's interior.

The VIRGO experiment (Fröhlich *et al.*, 1995) – besides measuring low degree intensity oscillations with unprecedented signal-to-noise ratio – provides the first high-precision observations of solar spectral irradiance at 402, 500 and 862 nm in parallel with total solar irradiance observations, allowing the study of simultaneous temporal changes in the near-UV, visible, and infrared ranges, and allow to determine the spectral distribution of total solar irradiance variations.

Figure 2 shows the results from a wavelet analysis for the $l = 0$, $n = 16 - 26$ modes from the VIRGO Sun PhotoMeters (SPM) blue channel. There is no clear correlation visible of the excitation of the different modes. Note the strong variations of the central frequency position of the various modes and the complicated mode structures with shifts and splittings. This is a result of phase wandering due to the stochastic excitation of the different modes, and is manifest as a power variation in different regions of the mean Lorentzian profile of the modes (Fröhlich *et al.*, 1997). This clearly demonstrates the danger of fitting Lorentzians to power spectra obtained from short time series, which inevitably will yield spurious frequency shifts. Tables of p-mode frequencies for modes $13 \leq n \leq 27$ and $0 \leq l \leq 7$ derived from SPM and Luminosity Oscillations Imager (LOI; Appourchaux *et al.*, 1997) power spectra can be found in Fröhlich *et al.* (1997).

The medium-l program of the Michelson Doppler Imager (MDI) instrument (Scherrer *et al.*, 1995) on board SOHO provides continuous observations of oscillation modes up to angular degree $l \approx 300$. The medium-l data are spatial averages of the full-disk Doppler velocity measured each minute. The initial results show that the noise in the medium-l data is substantially lower than in ground-based measurements, enabling the MDI team to detect lower amplitude modes and, thus, to extend the range of measured mode frequencies.

Kosovichev *et al.* (1997) determined the spherically symmetric structure of the Sun by inverting the mean frequencies of split mode multiplets ν_{nl} of the MDI medium-l data. Figure 2 shows the relative difference between the square of the sound speed in the Sun and reference model S of Christensen-Dalsgaard *et al.* (1996). The maximum difference between the model and the Sun is only 0.4%. Two features are particularly notable: (a) the narrow peak centred at $0.67\ R$, just beneath the convection zone, and (b) the sharp decrease of the sound speed compared to the model at the boundary of the energy-generating core ($\approx 0.25\ R$). The first feature most likely is due to a deficit of helium in this narrow region, possibly

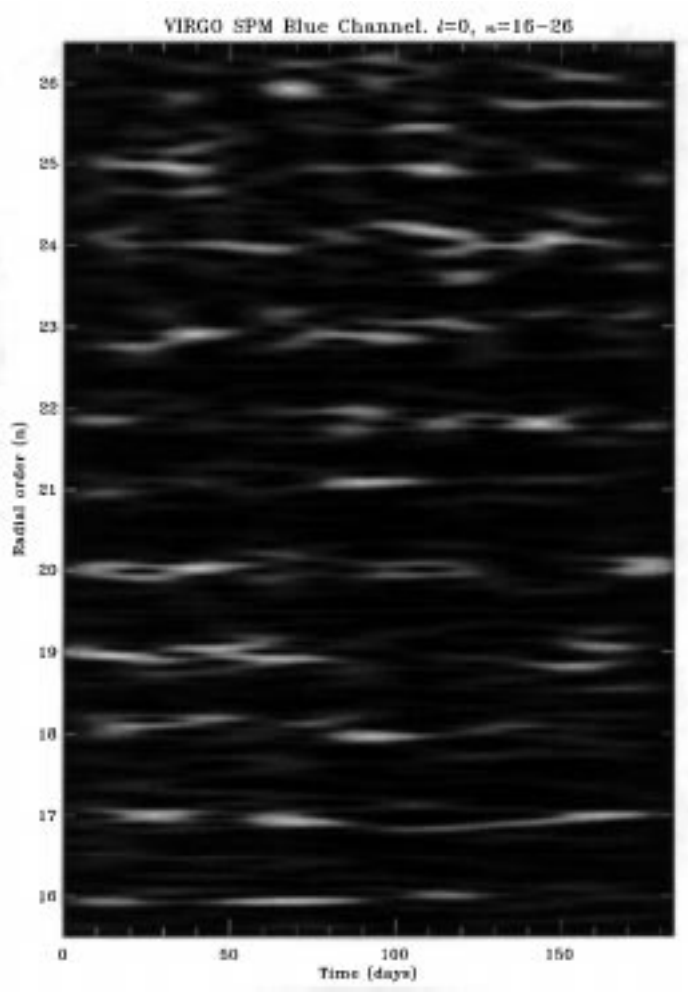

Figure 1. Wavelet analysis for modes $l = 0$, $n = 16 - 26$ from the VIRGO SPM blue channel. The frequency coverage for each radial order is 4 μHz (from Fröhlich *et al.*, 1997).

resulting from additional mixing in this layer of strong rotational shear. It was previously detected in the LOWL (Basu *et al.*, 1996) and GONG data (Gough *et al.*, 1996). The latter feature is not yet explained by theory. Kosovichev *et al.* (1997) speculate that the drop in sound speed may result from an overabundance of helium at the edge of the solar core. The steep increase of the sound speed towards the solar center can be explained if helium is less abundant than in the standard solar model, indicating a flatter helium abundance profile in the solar core than in the model. This variation in helium abundance may be due to errors in the rates of the nuclear reactions, to element diffusion, or to uncertainties in the equation of state and in radiative opacities. If the transition at the edge of the core is really as sharp as the initial analysis of MDI suggests, then material is redistributed in the

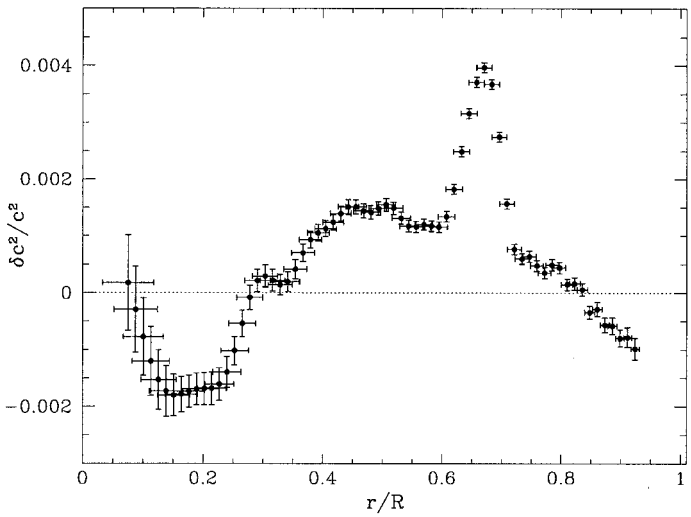

Figure 2. Relative differences between the squared sound speed in the Sun and a standard solar model as inferred from 2 months of MDI medium-*l* data. The horizontal bars indicate the spatial resolution, and the vertical bars are error estimates (from Kosovichev *et al.*, 1997).

core by macroscopic motion, possibly induced by the instability of ^{3}He burning, as first proposed by Dilke and Gough (1972). Detailed studies of this phenomenon are obviously very important for our understanding of stellar evolution, the nature of the solar neutrino problem, and for using the Sun as a laboratory for particle physics.

Figure 2 shows the internal rotation rate at three latitudes (0°, 30°, and 60°) as inferred by Kosovichev *et al.* (1997) from medium-*l* MDI data. This figure confirms previous findings that latitudinal differential rotation occurs only in the convection zone, that the radiative interior rotates almost rigidly, and that there is a thin shear layer near the surface. The feature particularly interesting in Figure 2 is the location of the transition layer (tachocline) between the differentially rotating convection zone and the rigidly rotating radiative zone. This transition layer is mostly located in the radiative zone, and is fairly thin (less than $0.1\ R$), at least at the equator. The sharp radial gradient of the angular velocity beneath the convection zone suggests that the sharp narrow peak seen in Figure 2 at $0.67\ R$ is due to rotationally induced turbulent mixing in the tachocline (Spiegel and Zahn, 1992). This layer is also likely to be the place where the solar dynamo operates.

Applying a new technique, called time-distance helioseismology (Duvall *et al.*, 1993), to high resolution MDI data, Duvall *et al.* (1997) and Kosovichev and Duvall (1997) were able to generate the first maps of horizontal and vertical flow velocities as well as sound speed variations in the convection zone just below the visible surface (Figure 2). Basically, this new technique measures the travel time of acoustic waves between various points on the surface. In a first approximation,

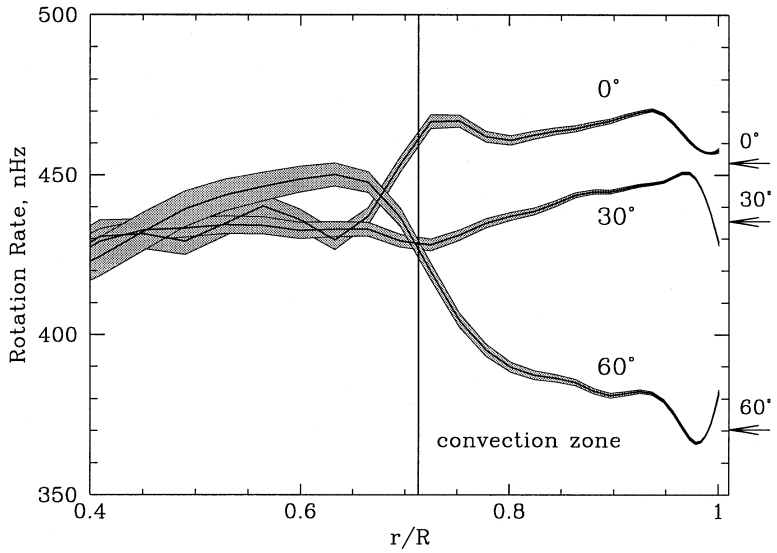

Figure 3. Solar rotation rate inferred from 2 months of MDI medium-l data as a function of radius at three latitudes (0°, 30°, and 60°). The formal errors are indicated by the shaded regions. The arrows indicate the Doppler rotation rate directly measured on the surface (from Kosovichev *et al.*, 1997).

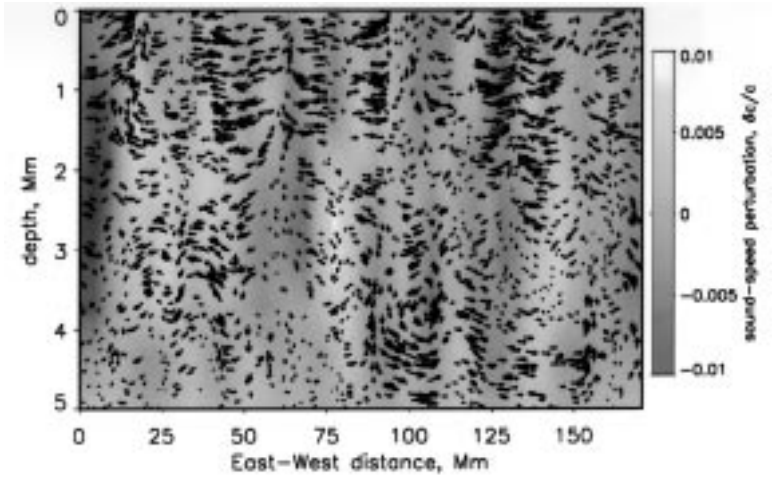

Figure 4. A vertical cut through the upper convection zone showing the subsurface flows and sound speed inhomogeneities. The flow field is shown as vectors (longest arrow 1.5 km s^{-1}) overlying the sound speed perturbations $\delta c/c$ (from Kosovichev and Duvall, 1997).

the waves can be considered to follow ray paths that depend only on a mean solar model, with the curvature of the ray paths being caused by the increasing sound speed with depth below the surface. The travel time is affected by various inhomogeneities along the ray path, including flow, temperature inhomogeneities, and magnetic fields. By measuring a large number of times between different locations and using an inversion method, it is possible to construct 3-dimensional maps of the subsurface inhomogeneities. In Figure 2 it appears that the pattern of horizontal motions near the surface only persists to a few Megameters in depth, indicating that supergranular convection cells may be much shallower than previously assumed. Additional observations at other times and locations will show whether the features that the map reveals are characteristic. Future observations will also allow the MDI team to make a 'movie' of this part of the convection zone so that they can observe how its structure changes over time.

3. The Solar Corona

Instruments on SOHO to observe the solar corona include imaging EUV telescopes, spectrometers, and coronagraphs. The imagers are used to study the morphology of the solar atmosphere, while the spectrometers are used to determine temperature, density, and line-of-sight velocity of specific volumes of the coronal plasma. SOHO's coronagraphs combine capabilities of both types of instrumentation to provide images and temperature, density and velocity measurements in the corona.

Images from the Extreme-Ultraviolet Imaging Telescope (EIT; Delaboudinière *et al.*, 1995) provide whole Sun pictures with a 5″ resolution (2.5″ pixels) at four wavelengths centered around spectral lines produced at about 80 000 K (He II 304 Å), 1 million K (Fe IX/X 171 Å), 1.5 million K (Fe XII 195 Å), and more than 2 million K (Fe XV 284 Å). Figure 2 shows a sample full disk EIT image in Fe XII 195 Å. In addition to the post-flare loops and prominence (in absorption) on the east limb, many features typical of the EUV corona are visible, including polar and transequatorial coronal holes, polar plumes, ephemeral active regions, and filament channels. Time series of images produced by EIT provide a superb view of the evolution of the lower corona, eruptive prominences and filaments, coronal holes, and coronal bright points.

SUMER – Solar Ultraviolet Measurements of Emitted Radiation (Wilhelm *et al.*, 1995) – is a high resolution normal incidence spectrograph providing stigmatic spectra in the range from 330 Å to 805 Å in 2nd order and from 660 Å to 1610 Å in 1st order (Figure 3). Line shifts and broadenings can be determined with subpixel accuracy down to 1 km s^{-1}. SUMER has already observed a wealth of solar phenomena such as filaments, prominences, bright points, explosive events, polar plumes, to name but a few. SUMER measurements of the line width of O VI 1032 Å in plume and inter-plume lane areas did not show any systematic dependence on

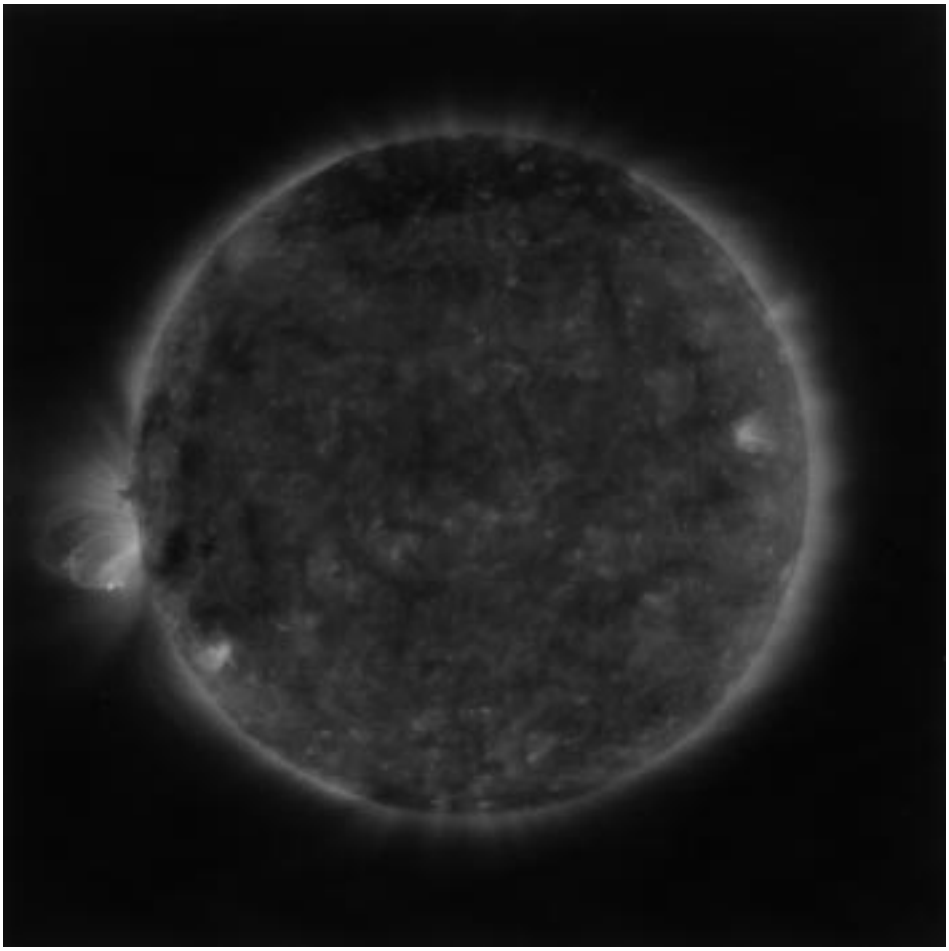

Figure 5. SOHO Extreme-ultraviolet Imaging Telescope (EIT) image in Fe XII 195 Å obtained on 1996 August 22 at 20:15 UT. In addition to the post-flare loops and prominence (in absorption) on the East limb, many features typical of the EUV corona are visible, including polar and transequatorial coronal holes, polar plumes, ephemeral active regions, and filament channels. (Courtesy of EIT Consortium)

height between 1 and 5 arcmin above the limb, neither was there a significant variation of the width for plume and inter-plume regions (Wilhelm *et al.*, 1997c). Wilhelm *et al.* (1997c) give 50 km s^{-1} for the measured Doppler width $\Delta\lambda_D$ of O VI 1032 Å at 1 arcmin above the limb, both in the center of a plume as well as in an inter-plume lane. Wilhelm *et al.* (1997c) also report electron density and temperature measurements in a coronal hole from 1 to 3 arcmin above the limb from Si VIII (1445/1440 Å) and Mg IX (750/706 Å) observations. They found – as expected – a strong dependence of the electron density, compatible with an exponential decrease with a scale height of approximately 1.1 arcmin (50000 km),

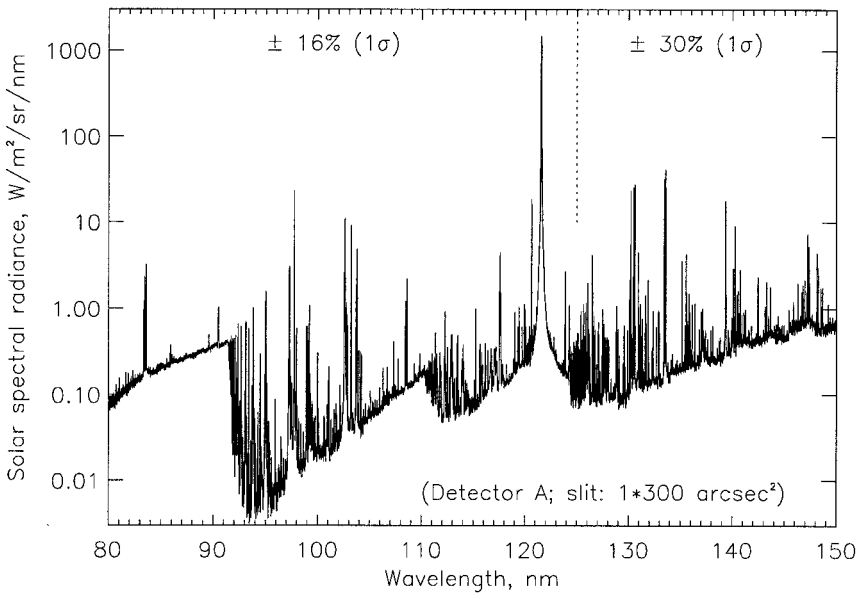

Figure 6. SUMER EUV spectral atlas in the range 800–1500 Å shown in first order converted to physical units using ground and onboard calibration data (from Wilhelm *et al.*, 1997b).

but the electron temperature does not vary significantly over the altitude range observed. Using the temperature sensitive line pair Mg IX (750/706 Å) they measured 8.4×10^5 K, 8.9×10^5 K, and 7.9×10^5 K at 1, 2, and 3 arcmin above the limb, respectively.

Due to the high spectral resolution and low noise of the instrument, SUMER has been able to detect faint lines not previously observed and, in addition, to determine their spectral profiles. SUMER has already recorded more than 2000 EUV emission lines and many new identifications have been made on the disk and in the corona (Curdt *et al.*, 1997; Feldman *et al.*, 1997).

CDS, the Coronal Diagnostic Spectrometer (Harrison *et al.*, 1995) is a twin spectrometer operating in the EUV range from 151 to 785 Å. A first set of line identifications from CDS spectral atlas measurements covering lines in the temperature range $\log T = 4.3$ to 3.6 with numerous density diagnostic line pairs is given in Harrison *et al.* (1997). Analysis of spectral line profiles recorded with the CDS revealed significant flows of plasma taking place in active region loops, both at coronal and transition region temperatures (Brekke *et al.*, 1997). Wavelength shifts in the coronal lines Mg IX 368 Å and Mg X 624 Å corresponding to upflows in the plasma reaching velocities of 50 km s^{-1} have been observed in an active region. Flows reaching 100 km s^{-1} have been observed in spectral lines formed at transition region temperatures, i.e., O V 629 Å and O III 599 Å (Figure 3), demonstrating that both the transition region and the corona are clearly dynamic in nature. Velocities of this magnitude have never previously been observed in

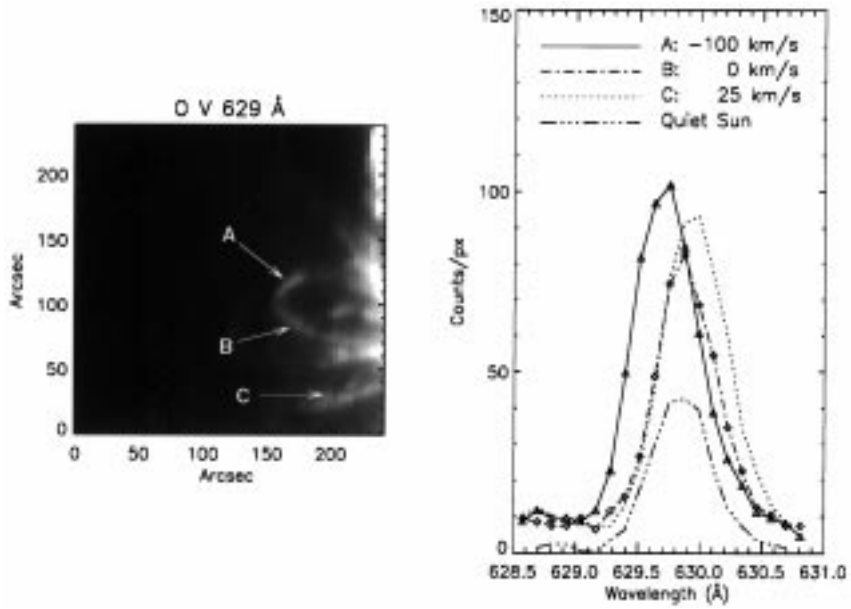

Figure 7. Active region loop system above the east limb observed in O V 629 Å on July 27 1996. The line profiles from three different spatial locations (A, B, C) are displayed in the right panel together with a quiet Sun disk center profile (from Brekke *et al.*, 1997)

coronal lines except in explosive events and flares. The new data obtained with CDS therefore promise to put severe constraints on existing models of flows and energy balance in the solar atmosphere.

CDS has also observed strong high velocity events occurring simultaneously in many lines from He I to Fe XVI, i.e., over a temperature range from 20 000 K to 2.5 million K (Fludra, priv. comm.). Such a finding has never been reported before. It is a challenge to theoretical models and may cause a re-examination of the contribution of explosive events to coronal heating. On the other hand, the 'explosive event' discussed in Brekke *et al.* (1997), characterized by a high velocity dispersion of 300–400 km s^{-1}, showed up strongly only in O III 599 Å and Ne VI 562 Å, whereas in Mg VI 349 Å, Mg IX 368 Å, and Mg X 624 Å only a weak signature could be observed, and no trace of this event was visible in Si XII 520 Å and Fe XVI 335 Å.

First electron density and temperature distributions from CDS EUV observations have been determined by Mason *et al.* (1997), for a variety of solar features.

Two coronagraphs (LASCO and UVCS) make observations of the extended corona and the solar wind at its inception. For the first time it is possible to observe the expansion of the solar corona into the solar wind up to 32 solar radii (LASCO) and to perform plasma diagnostic spectroscopy up to 10 solar radii (UVCS).

LASCO, the Large Angle Spectroscopic Coronagraph (Brueckner *et al.*, 1995), uses a set of three nested coronagraphs to observe the outer solar atmosphere from

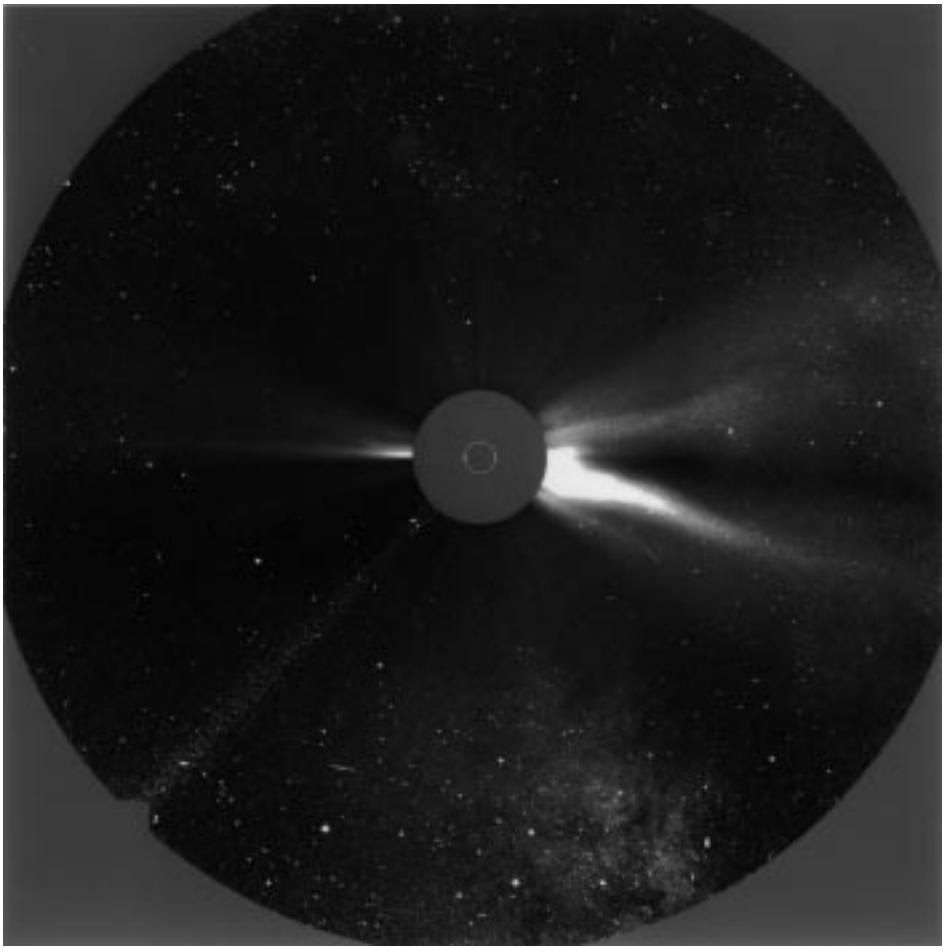

Figure 8. White light image of the extended corona taken by the LASCO C3 coronagraph on 24 December 1996, 02:50 UT. The field-of-view of this instrument encompasses 32 solar diameters (45 million kilometers at the distance of the Sun, or half the diameter of the orbit of Mercury). Time-lapse sequences of these images show the cloudy solar wind flowing out of the Sun in front of the Milky Way. This particular image was taken when the Sun was located in the constellation Sagittarius. (Courtesy of LASCO consortium)

the solar limb out to a distance of 32 solar radii (Figure 3). Time-lapse sequences of white-light images obtained with the LASCO C-2 and C3 coronagraphs give the impression of a continual outflow of material from the Sun, presumably resulting from Thomson scattered emission from inhomogeneities in the solar wind (Sheeley *et al.*, 1997). By tracking several tens of the most prominent features Sheeley *et al.* (1997) found that these features move radially outward with their speed typically doubling from 150 km s^{-1} near 5 $R_\odot$ to 300 km s^{-1} near 25 $R_\odot$. The individual speed profiles $v(r)$ of these features cluster around a nearly parabolic path characterized by a nearly constant acceleration of about 4 m s^{-2} through most of the

30 $R_\odot$ field-of-view, in contrast to similar measurements for coronal mass ejections. Sheeley *et al.* (1997) therefore concluded that they are seeing 'bits of helmet streamers being torn away by the slow solar wind and carried passively outward as tracers of the wind speed'. They further used the observed speed profile of the slow solar wind as an empirical constraint on the classic solar wind equations, enabling them to determine both the temperature (and thus the sound speed) as a function of radial distance from the Sun as well as the location of the sonic point. The observed speed profiles are consistent with an isothermal solar wind expansion at a temperature of about 1.1 MK ($v_s \approx 130 - 140$ km s^{-1}) and a sonic point near 5 $R_\odot$ (Sheeley *et al.*, 1997).

Simnett *et al.* (1997) analysed two coronal mass ejections (CMEs) observed by LASCO which moved out into the interplanetary medium as disconnected plasmoids. They noted a strong acceleration of the plasmoids around 5 to 6 solar radii which they interprete as a manifestation of the source surface of the slow solar wind. They also found that in both events the rising plasmoid is connected back to the Sun by a straight, bright ray, which they interprete as a signature of a neutral sheet.

From LASCO C-1 observations of the green emission line corona (Fe XIV 5303 Å) Schwenn *et al.* (1997) found that bright, apparently closed, loop systems are almost permanently present at 30° to 40° latitude. Their helmet-like extensions are bent towards the equator where they merge further out into one large equatorial streamer sheet which is visible out to 32 solar radii. At mid latitudes a more diffuse and time variable pattern is visible, well separated from the high-latitude loop system. No green line emission is observed in the polar coronal holes.

The Ultraviolet Coronagraph Spectrometer (UVCS) on board SOHO performs ultraviolet spectroscopy combined with plasma diagnostic analysis techniques to obtain a detailed empirical description of the extended solar corona beyond 1.5 $R_\odot$ where the primary solar wind acceleration takes place (Kohl *et al.*, 1995). UVCS has obtained the first ultraviolet images of the extended solar corona above two solar radii from the center of the Sun. Antonucci *et al.* (1997), applying the Doppler dimming technique (Beckers and Chipman, 1974) to UVCS measurements of the O VI line pair at 1032/1037 Å, found evidence for solar wind acceleration in open field line regions both at the pole and just outside equatorial streamers, with velocities reaching 100 km s^{-1} at about 2 $R_\odot$ in polar regions and within $2.2 - 2.6$ $R_\odot$ outside streamers. The RMS velocities derived from the line-of-sight velocity distribution provide a clear signature for open field line regions. O VI 1032 Å line profiles in coronal holes, and in general in closed field regions with open magnetic field lines, are much broader than in closed field line regions. Line-of-sight velocities in polar regions were found to be within 100–230 km s^{-1} between 1.5 and 2.6 $R_\odot$, and within 100–140 km s^{-1} between 1.6 and 3.1 $R_\odot$ outside the border of a streamer (Antonucci *et al.*, 1997). Closed field line regions inside streamers have much reduced velocities (< 70 km s^{-1}). These RMS velocities include both thermal and non-thermal motions along the line-of-sight. These results there-

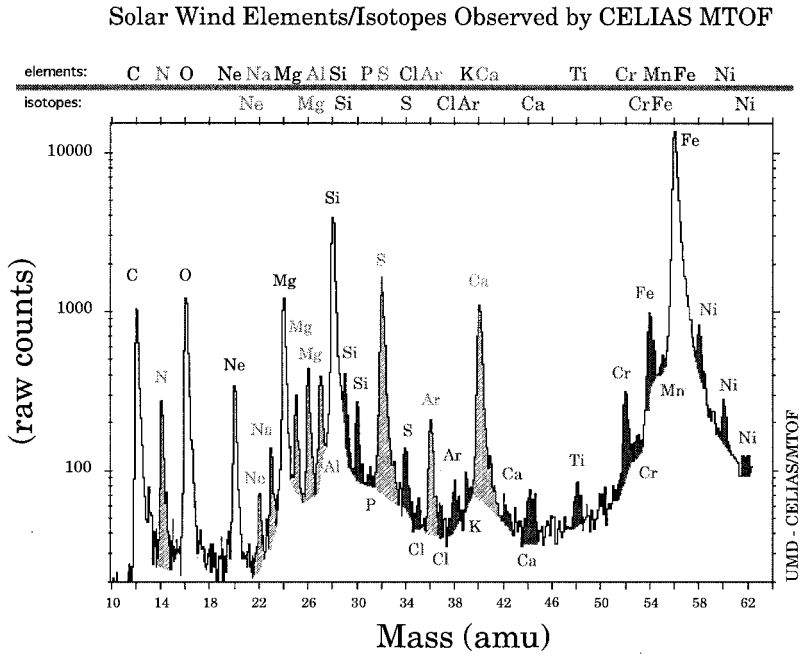

Figure 9. Element and isotope spectrum as obtained with the MTOF sensor of CELIAS. Many elements such as phosphorus, chlorine, potassium, titanium, chromium, and nickel are being measured in the solar wind for the first time. (Courtesy of CELIAS consortium)

fore indicate that open magnetic field lines are the site of enhanced non-thermal and/or thermal motions. The enhanced motions might be related to the presence of Alfvén waves, detectable as non-thermal motions and/or their dissipation resulting in thermal motions of the ions.

4. The Solar Wind

Three instruments measure the composition and energy spectrum of particles in the Solar Wind. The Charge, Element, Isotope Analysis System (CELIAS) investigation on SOHO is a multi-sensor experiment consisting of three sensors that measure the composition and energy spectra of plasma (solar wind) and energetic ions of solar, interplanetary, and interstellar origin, and a fourth sensor for monitoring the absolute EUV (extreme ultraviolet) flux from the Sun (Hovestadt *et al.*, 1995). The CELIAS solar wind mass spectrometer (MTOF, Mass Time-of-Flight Sensor) has unprecedented mass resolution for solar wind composition studies, and has already measured rare elements and isotopes that were previously not resolvable from more abundant neighbouring species, or were not previously observable at all. For example, as seen in Figure 3, the elements of sulphur, argon, and calcium

are now easily distinguished from the neighbouring species of silicon and iron, as is nitrogen from carbon and oxygen. The rare elements phosphorus, chlorine, potassium, titanium, chromium, manganese, and nickel are being measured in the solar wind for the first time. Some of these elements (P, Cl, K, Ti, Cr, and Mn) have no coronal spectroscopic measurements available. The determination of the elemental abundances of these rarer species allow to fill in the 'blanks' of the solar wind versus photospheric abundance tables. This is important in obtaining a better analysis of the solar wind feeding and acceleration processes in the chromosphere and inner corona. The solar wind and coronal abundances indicate an ordering of relative abundance enhancement (or depletion) to photospheric values partially correlated with the first ionization potential (FIP) of the element (the so-called 'FIP effect'; e.g., Mayer, 1993). Since these newly observed elements have different properties (such as first ionization potentials, first ionization times, charge state equilibrium times, atomic mass, etc.), knowledge of their relative abundances serve as diagnostic tools for determining conditions in the chromosphere/transition region, where ions which eventually become the solar wind are separated from neutrals.

The Comprehensive SupraThermal and Energetic Particle analyzer (COSTEP; Müller-Mellin *et al.*, 1995) measures electrons from 45 KeV to 10 MeV and hydrogen and helium nuclei from 45 KeV to 53 MeV. Due to the phase in the solar activity cycle close to solar minimum the sun was extremely quiet during the first phase of the SOHO mission. Therefore, except for isolated small particle events, only steady state processes could be studied so far with the COSTEP instrument. With increasing solar activity specific events such as flares and CMEs will become much more frequent, allowing the COSTEP team to investigate the energy release and particle acceleration processes in the solar atmosphere.

Of the solar wind particle detectors on SOHO, the Energetic and Relativistic Nuclei and Electron experiment (ERNE; Torsti *et al.*, 1995) covers the highest energies, roughly from 1 MeV/n to 500 MeV/n. The first energetic particle event observed by ERNE occurred on 20–25 January, 1996. Torsti *et al.* (1997a) concluded that the particles were accelerated in a corotating interaction region (CIR). A similar event was observed on 6–12 May, almost exactly four solar rotation periods after the January event. The first solar originated particle events observed by ERNE occurred on 22–23 April and 14–17 May, 1996. The first one resulted from an active region near the west limb of the Sun, and no ^{3}He ions were detected. The May 14–15 event, in contrast, was extremely ^{3}He rich: it had a ^{3}He-to-proton ratio of 1.5 ± 0.6 and a ^{3}He-to ^{4}He ratio as high as ≈ 8 (Torsti *et al.*, 1997a).

ERNE has also measured the energy spectra of the anomalous cosmic ray components of helium, nitrogen and oxygen (Torsti *et al.*, 1997b). The peak intensities found are at the same level as two solar cycles ago in 1977, but significantly higher than in 1986, providing evidence for a 22-year solar cycle modulation. The spectra of nitrogen and oxygen appear to be somewhat broader than in 1977.

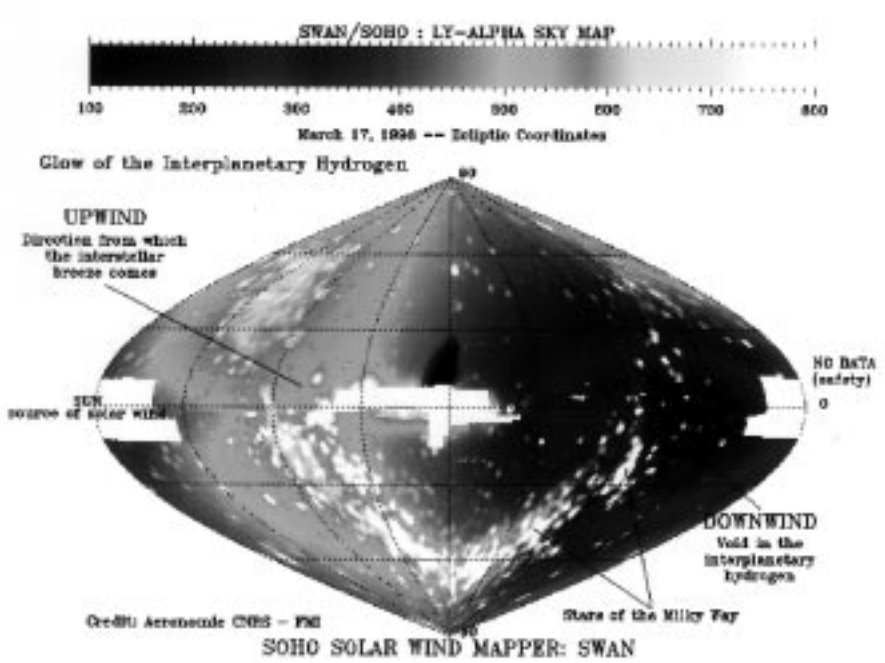

Figure 10. Full sky Lyman-α map in ecliptic co-ordinates as recorded by the SWAN instrument. Two areas were not covered for safety reasons, around the Sun and around the anti-solar direction. Intensity is given in counts per second per pixel (one square degree), which corresponds to 1.3 Rayleigh. Numerous hot UV stars can be identified, tracing the galactic plane. The rest of the ubiquitous emission is due to solar UV Lyman-α photons, backscattered by Hydrogen atoms in the solar system. A detailed analysis of such Lyman-α maps allows to determine the latitude distribution of the solar wind mass flux. (Courtesy of SWAN consortium)

To determine the dynamic change of the large-scale solar wind flow, SWAN (Solar Wind ANisotropies; Bertaux *et al.*, 1995) monitors the heliographic latitude distribution of the solar wind flow by mapping the Lyman-α emission from resonantly scattering interstellar hydrogen atoms (Figure 4). Numerous hot stars can be identified, tracing the galactic plane. The rest of the ubiquitous emission is due to solar UV Lyman-α photons, backscattered by hydrogen atoms in the solar system. These H atoms are coming from interstellar space, approaching the Sun down to about 2 AU in the direction of the incoming flow ($\lambda = 254°$, $\beta = 7°$). A maximum of Lyman-α intensity surrounds this upwind direction. In the opposite direction, the emission is weaker by a factor of about 3.5, because most atoms have been destroyed by charge-exchange with solar wind protons, creating a cavity void of hydrogen atoms in the downwind direction. A detailed analysis of the variations with time of such Lyman-α maps allows to determine the latitude distribution of the solar wind mass flux. At the present time of a quiet Sun, the SWAN sky maps indicate a situation of increased solar wind flux around the Sun's equator in the

ecliptic plane, confirming out-of ecliptic in-situ measurements by Ulysses (Phillips *et al.*, 1995).

5. Conclusions

Already during its first few months of operation, SOHO has obtained exciting new results, seeing features on the Sun never seen before, or never seen so clearly, and providing new insights to fundamental unsolved problems all the way from the Sun's deep interior out to the far reaches of the solar wind. It should be noted, though, that all the results presented in this paper are early results from individual instruments, while SOHO was conceived as an integrated package of complementary instruments to be operated in a coordinated programme, such that their measurements would provide a complementary and comprehensive data set for the study of the complex physical processes in the solar atmosphere, in the solar wind, and in the solar interior. One therefore expects that the main results from SOHO will come from joint, correlative analysis of coordinated observations. And this in fact is happening: A significant fraction of the observing time of the SOHO instruments is devoted to joint observing programmes (so-called 'JOPs'). JOPs are an effort by the SOHO Science Planning Working Group to produce coherent observing plans and sequences to maximize the scientific return of the various SOHO instruments by coordinating individual observing plans for the study of specific solar phenomena. Many JOPs involve collaborations with other ground-based or space based observatories. In addition to the numerous SOHO internal JOPs, there have been already more than 80 campaigns with other ground-based observatories and/or the Soft X-ray Telescope (SXT) onboard Yohkoh (Ogawara *et al.*, 1991), some of which were large multi-site efforts involving observatories all around the world.

More information about the SOHO mission is available on the World Wide Web at *http:\\sohowww.nascom.nasa.gov* with links to

- In-depth descriptions of the mission and the instruments
- SOHO gallery
- SOHO archive
- SOHO software
- Latest images (including daily solar synoptic images from numerous ground-based observatories around the world and from Yohkoh/SXT)
- Observing plans and targets
- Campaign and JOP lists

and many other useful links to relevant pages in solar physics, space plasma physics and astrophysics.

Acknowledgements

I am grateful to all the colleagues who provided me with preprints and digital versions of figures for this paper, in particular to Sasha Kosovichev, Paal Brekke, Claus Fröhlich, Toni Galvin, Joe Gurman, Fred Ipavich, Scott Paswaters, Eric Quemerais, and Klaus Wilhelm. SOHO is a mission of international cooperation between ESA and NASA.

References

Antonucci, E., Noci, G., Kohl, J.L., Tondello, G., Huber, M.C.E., Giordano, S., Benna, C., Ciaravella, A., Fineschi, S., Gardner, L.D., Martin, R., Michels, J., Naletto, G., Nicolosi, P., Panasyuk, A., Raymond, C.J., Romoli, M., Spadaro, D., Strachan, L. and van Ballegooijen, A.: 1997, in: J.C. Del Toro Iniesta *et al.* (eds), *Advances in the Physics of Sunspots*, ASP Conf. Series, in press.

Appourchaux, T., Andersen, B.N., Fröhlich, C., Jiménez, A., Telljohann, U. and Wehrli, C.: 1997, *Sol. Phys.* **170**, 27–41.

Basu, S., Christensen-Dalsgaard, J., Schou, J., Thompson, M.J. and Tomczyk, S.: 1996, *Bull. Astron. Soc. India* **24**, 147.

Beckers, J.M. and Chipman, E.: 1974, *Sol. Phys.* **34**, 151.

Bertaux, J.L., Kyrölä, E., Quémerais, E., Pellinen, R., Lallement, R., Schmidt, W., Berthé, M., Dimarellis, E., Goutail, J.P., Taulemesse, C., Bernard, C., Leppelmeier, G., Summanen, T., Hannula, H., Huomo, H., Kehlä, V., Korpela, S., Leppälä, K., Strömmer, E., Torsti, J., Viherkanto, K., Hochedez, J.F., Chretiennot, G., Peyroux, R. and Holzer, T.: 1995, *Sol. Phys.* **162**, 403–439.

Brekke, P., Kjeldseth-Moe, O., Brynildsen, N., Maltby, P., Haugan, S.V.H., Harrison, R.A., Thompson, W.T. and Pike, C.D.: 1997, *Sol. Phys.* **170**, 163–177.

Brueckner, G.E., Howard, R.A., Koomen, M.J., Korendyke, C.M., Michels, D.J., Moses, J.D., Socker, D.G., Dere, K.P., Lamy, P.L., Llebaria, A., Bout, M.V., Schwenn, R., Simnet, G.M., Bedford, D.K. and Eyles, C.J.: 1995, *Sol. Phys.* **162**, 357–402.

Christensen-Dalsgaard, J., Däppen, W., Ajukov, S.V., Anderson, E.R., Antia, H.M., Basu, S., Baturin, V.A., Berthomieu, G., Chaboyer, B., Chitre, S.M., Cox, A.N., Demarque, P., Donatowicz, J., Dziembowski, W.A., Gabriel, M., Gough, D.O., Guenther, D.B., Guzik, J.A., Harvey, J.W., Hill, F., Houdek, G., Iglesias, C.A., Kosovichev, A.G., Leibacher, J.W., Morel, P., Proffitt, C.R., Provost, J., Reiter, J., Rhodes Jr., E.J., Rogers, F.J., Roxburgh, I.W., Thompson, M.J. and Ulrich, R.K.: 1996, *Science* **272**, 1286.

Curdt, W., Feldman, U., Laming, J.M., Wilhelm, K., Schühle, U. and Lemaire, P.: 1997, *Astron. Astrophys.*, in press.

Delaboudinière, J.-P., Artzner, G.E., Brunaud, J., Gabriel, A.H., Hochedez, J.F., Millier, F., Song, X.Y., Au, B., Dere, K.P., Howard, R.A., Kreplin, R., Michels, D.J., Moses, J.D., Defise, J.M., Jamar, C., Rochus, P., Chauvineau, J.P., Marioge, J.P., Catura, R.C., Lemen, J.R., Shing, L., Stern, R.A., Gurman, J.B., Neupert, W.M., Maucherat, A., Clette, F., Cugnon, P. and Van Dessel, E.L.: 1995, *Sol. Phys.* **162**, 291–312.

Dilke, F.W.W. and Gough, D.O.: 1972, *Nature* **240**, 262.

Domingo, V., Fleck, B. and Poland, A.I.: 1995, *Sol. Phys.* **162**, 1–37.

Duvall, T.L., Jefferies, S.M., Harvey, J.W. and Pomerantz, M.A.: 1993, *Nature* **362**, 430.

Duvall, T.L., Kosovichev, A.G., Scherrer, P.H., Bogart, R.S., Bush, R.I., De Forest, C., Hoeksema, J.T., Schou, J., Saba, J.L.R., Tarbell, T.D., Title, A.M., Wolfson, C.J. and Milford, P.N.: 1997, *Sol. Phys.* **170**, 63–73.

Feldman, U., Behring, W.E., Curdt, W., Schühle, U., Wilhelm, K. and Lemaire, P.: 1997, *Astrophys. J. Suppl.*, in press.

Fleck, B., Domingo, V. and Poland, A.I. (eds): 1995, The SOHO Mission, *Sol. Phys.* **162**, Nos. 1–2.

Fröhlich, C., Romero, J., Roth, H., Wehrli, C., Andersen, B.N., Appourchaux, T., Domingo, V., Telljohann, U., Berthomieu, G., Delache, P., Provost, J., Toutain, T., Crommelynck, D.A., Chevalier, A., Fichot, A., Daeppen, W., Gough, D., Hoeksema, T., Jimenez, A., Gomez, M.F., Herreros, J.M., Roca Cortes, T., Jones, A.R., Pap, J.M. and Wilson, R.C.: 1995, *Sol. Phys.* **162**, 101–128.

Fröhlich, C., Andersen, B.N., Appourchaux, T., Berthomieu, G., Crommelynck, D.A., Domingo, V., Fichot, A., Finsterle, W., Gomez, M.F., Gough, D., Jiménez, A., Leifsen, T., Lombaerts, M., Pap, J.M., Provost, J., Roca Cortés, T., Romero, J., Roth, H., Sekii, T., Telljohann, U., Toutain, T. and Wehrli, C.: 1997, *Sol. Phys.* **170**, 1–25.

Gabriel, A.H., Grec, G., Charra, J., Robillot, J.-M., Roca Cortes, T., Turck-Chieze, S., Bocchia, R., Boumier, P., Cantin, M., Cespedes, E., Cougrand, B., Cretolle, J., Dame, L., Decaudin, M., Delache, P., Denis, N., Duc, R., Dzitko, H., Fossat, E., Fourmond, J.-J., Garcia, R.A., Gough, D., Grivel, C., Herreros, J.M., Lagardere, H., Moalic, J.-P., Palle, P.L., Petrou, N., Sanchez, M., Ulrich, R. and Van Der Raay, H.B.: 1995, *Sol. Phys.* **162**, 61–99.

Gough, D.O., Kosovichev, A.G., Toomre, J., Anderson, E., Antia, H.M., Basu, S., Chaboyer, B., Chitre, S.M., Christensen-Dalsgaard, J., Dziembowski, W.A., Eff-Darwich, A., Elliott, J.R., Giles, P.M., Goode, P.R., Guzik, J.A., Harvey, J.W., Hill, F., Leibacher, J.W., Monteiro, M.J.P.F.G., Richard, O., Sekii, T., Shibahashi, H., Takata, M., Thompson, M.J., Vauclair, S. and Vorontsov, S.V.: 1996, *Science* **272**, 1296.

Harrison, R.A., Sawyer, E.C., Carter, M.K., Cruise, A.M., Cutler, R.M., Fludra, A., Hayes, R.W., Kent, B.J., Lang, J., Parker, D.J., Payne, J., Pike, C.D., Peskett, S.C., Richards, A.G., Culhane, J.L., Norman, K., Breeveld, A.A., Breeveld, E.R., Al Janabi, K.F., McCalden, A.J., Parkinson, J.H., Self, D.G., Thomas, P.D., Poland, A.I., Thomas, R.J., Thompson, W.T., Kjeldseth-Moe, O., Brekke, P., Karud, J., Maltby, P., Aschenbach, B., Braeuninger, H., Kuehne, M., Hollandt, J., Siegmund, O.H.W., Huber, M.C.E., Gabriel, A.H., Mason, H.E. and Bromage, B.J.I.: 1995, *Sol. Phys.* **162**, 233–290.

Harrison, R.A., Fludra, A., Pike, C.D., Payne, J., Thompson, W.T., Poland, A.I., Breeveld, E.R., Breeveld, A.A., Culhane, J.L., Kjeldseth-Moe, O., Huber, M.C.E. and Aschenbach, B.: 1997, *Sol. Phys.* **170**, 123–141.

Hovestadt, D., Hilchenbach, M., Bürgi, A., Klecker, B., Laeverenz, P., Scholer, M., Grünwaldt, H., Axford, W.I., Livi, S., Marsch, E., Wilken, B., Winterhoff, H.P., Ipavich, F.M., Bedini, P., Coplan, M.A., Galvin, A.B., Gloeckler, G., Bochsler, P., Balsinger, H., Fischer, J.,Geiss, J., Kallenbach, R., Wurz, P., Reiche, K.-U., Gliem, F., Judge, D.L., Ogawa, H.S., Hsieh, K.C., Moebius, E., Lee, M.A., Managadze, G.G., Verigin, M.I. and Neugebauer, M.: 1995, *Sol. Phys.* **162**, 441–481.

Kohl, J.L., Esser, R., Gardner, L.D., Habbal, S., Daigneau, P.S., Dennis, E.F., Nystrom, G.U., Panasyuk, A., Raymond, J.C., Smith, P.L., Strachan, L., Van Ballegooijen, A.A., Noci, G., Fineschi, S., Romoli, M., Ciaravella, A., Modigliani, A., Huber, M.C.E., Antonucci, E., Benna, C., Giordano, S., Tondello, G., Nicolosi, P., Naletto, G., Pernechele, C., Spadaro, D., Poletto, G., Livi, S., Von Der Luehe, O., Geiss, J., Timothy, J.G., Gloeckler, G., Allegra, A., Basile, G., Brusa, R., Wood, B., Siegmund, O.H.W., Fowler, W., Fisher, R. and Jhabvala, M.: 1995, *Sol. Phys.* **162**, 313–356.

Kosovichev, A.G. and Duvall, T.L.: 1997, in: J. Christensen-Dalsgaard and F. Pijpers (eds), *Solar Convection and Oscillations and Their Relationship*, Proc. of SCORe'96 Workshop, Aarhus, Denmark, Kluwer Academic Publishers, in press.

Kosovichev, A.G., Schou, J., Scherrer, P.H., Bogart, R.S., Bush, R.I., Hoeksema, J.T., Aloise, J., Bacon, L., Burnette, A., De Forest, C., Giles, P.M., Leibrand, K., Nigam, R., Rubin, M., Scott, K., Williams, S.D., Basu, S., Christensen-Dalsgaard, J., Däppen, W., Rhodes, E.J., Duvall, T.L., Howe, R., Thompson, M.J., Gough, D.O., Sekii, T., Toomre, J., Tarbell, T.D., Title, A.M., Mathur,

D., Morrison, M., Saba, J.L.R., Wolfson, C.J., Zayer, I. and Milford, P.N.: 1997, *Sol. Phys.* **170**, 43–61.

Lemaire, P., Wilhelm, K., Curdt, W., Schühle, U., Marsch, E., Poland, A.I., Jordan, S.D., Thomas, R.J., Hassler, D.M., Vial, J.-C., Kḧne, M., Huber, M.C.E., Siegmund, O.H.W., Gabriel, A., Timothy, J.G. and Grewing, M.: 1997, *Sol. Phys.* **170**, 105–122.

Mason, H.E., Young, P.R., Pike, C.D., Harrison, R.A., Fludra, A., Bromage, B.J.I. and Del Zanna, G.: 1997, *Sol. Phys.* **170**, 143–161.

Müller-Mellin, R., Kunow, H., Fleissner, V., Pehlke, E., Rode, E., Roeschman, N., Scharmberg, C., Sierks, H., Rusznyak, P., McKenna-Lawlor, S., Elendt, I., Sequeiros, J., Meziat, D., Sanchez, S., Medina, J., Del Peral, L., Witte, M., Marsden, R. and Henrion, J.: 1995, *Sol. Phys.* **162**, 483–504.

Mayer, J.-P.: 1993, *Adv. Space Res.* **13**, 377.

Ogawara, Y., Takano, T., Kato, T., Kosugi, T., Tsuneta, S., Watanabe, T., Kondo, I. and Uchida, Y.: 1995, *Sol. Phys.* **136**, 1.

Phillips, J.L., Bame, S.J., Barnes, A., Barraclough, B.L., Feldman, W.C., Goldstein, B.E., Gosling, J.T., Hoogeveen, G.W., McComas, D.J., Neugebauer, M. and Suess, S.T.: 1995, *Geophys. Res. Lett.* **22**, 3301.

Scherrer, P.H., Bogard, R.S., Bush, R.I., Hoeksema, J.T., Kosovichev, A.G., Schou, J., Rosenberg, W., Springer, L., Tarbell, T.D., Title, A., Wolfson, C.J. and Zayer, I., The MDI Engineering Team: 1995, *Sol. Phys.* **162**, 129–188.

Schwenn, R., Inhester, B., Plunkett, S.P., Epple, A., Podlipnik, B., Bedford, D.K., Bout, M.V., Brueckner, G.E., Dere, K.P., Eyles, C.J., Howard, R.A., Koomen, M.J., Korendyke, C.M., Lamy, P., Llebaria, A., Michels, D.J., Moses, J.D., Moulton, N.E., Paswaters, S.E., Simnett, G.M., Socker, D.G., St. Cyr, O.C., Tappin, S.J. and Wang, D.: 1997, *Sol. Phys.* **173**, in press.

Sheeley, N.R., Wang, Y.-M., Hawley, S.H., Brueckner, G.E., Dere, K.P., Howard, R.A., Koomen, M.J., Korendyke, C.M., Michels, D.J., Paswaters, S.E., Socker, D.G., St. Cyr, O.C., Wang, D., Lamy, P.L., Llebaria, A., Schwenn, R., Simnett, G.M., Plunkett, S. and Biesecker, D.A.: 1997, *Astrophys. J.*, in press.

Simnett, G.M., Tappin, S.J., Plunkett, S.P., Medford, D.K., Eyles, C.J., St. Cyr, O.C., Howard, R.A., Brueckner, G.E., Michels, D.J., Moses, J.D., Socker, D., Dere, K.P., Korendyke, C.M., Paswaters, S.E., Wang, D., Schwenn, R., Lamy, P., Llebaria, A. and Bout, M.V.: 1997, *Sol. Phys.* **173**, in press.

Spiegel, E.A. and Zahn, J.-P.: 1992, *Astron. Astrophys.* **265**, 106.

Torsti, J., Valtonen, E., Lumme, M., Peltonen, P., Eronen, T., Louhola, M., Riihonen, E., Schultz, G., Teittinen, M., Ahola, K., Holmlund, C., Kelhae, V., Leppaelae, K., Ruuska, P. and Stroemmer, E.: 1995, *Sol. Phys.* **162**, 505–531.

Torsti, J., Valtonen, E., Kocharov, L.G., Vainio, R., Riihonen, E., Anttila, A., Laitinen, T., Teittinen, M. and Kuusela, J.: 1997a, *Sol. Phys.* **170**, 179–191.

Torsti, J., Valtonen, E., Anttila, A., Vainio, R., Mäkelä, P., Riihonen, E. and Teittinen, M.: 1997b, *Sol. Phys.* **170**, 193–205.

Wilhelm, K., Curdt, W., Marsch, E., Schühle, U., Lemaire, P., Gabriel, A., Vial, J.-C., Grewing, M., Huber, M.C.E., Jordan, S.D., Poland, A.I., Thomas, R.J., Kühne, M., Timothy, J.G., Hassler, D.M. and Siegmund, O.H.W.: 1995, *Sol. Phys.* **162**, 189–231.

Wilhelm, K., Lemaire, P., Curdt, W., Schühle, U., Marsch, E., Poland, A.I., Jordan, S.D., Thomas, R.J., Hassler, D.M., Huber, M.C.E., Vial, J.-C., Kühne, M., Siegmund, O.H.W., Gabriel, A., Timothy, J.G., Grewing, M., Feldman, U., Hollandt, J. and Brekke, P.: 1997a, *Sol. Phys.* **170**, 75–104.

Wilhelm, K., Lemaire, P., Dammasch, I.E., Hollandt, J., Schühle, U., Curdt, W., Kucera, T. and Hassler, D.M.: 1997b, *Geophys. Res. Lett.*, in press.

Wilhelm, K., and the SUMER team: 1997c, in: J.C. Del Toro Iniesta *et al.* (eds), *Advances in the Physics of Sunspots*, ASP Conf. Series, in press.